The Design of a Two-Wheeled Auto-Balancing Robot under Impulse Interruption

Kanchit Pawananont[1] and **Kritchanan Charoensuk**[2†], Non-members

ABSTRACT

The innovation of two-wheeled balancing robots affects human life in different ways. Immense research continues to be undertaken to make such robots cheap, efficient, and reliable. Essentially, autonomous mobile robots are two-wheeled, vertical, and self-balancing. The robot's control system and automation application are intergraded with daily human life. Autonomy is applied to vehicles such as mobile robots, referred to as a vehicle capable of independent motion. Mobile robots can be used in various applications such as exploration, the food industry, home service, security, logistics, and many more. Moreover, it can be classified into four types: locomotion, perception, cognition, and navigation. In this work, the two-wheel, auto-balancing robot is investigated. The two-wheeled robot cannot operate without a controller and is susceptible to interruption and lean-to plunging outside the field. The PD controller, linear quadratic regulator (LQR), sliding mode control (SMC), and fuzzy logic control (FLC) can be used to set the robot into a stable upright position in the rotation angle condition. In this research, four control strategies are compared to obtain the solid validation of a two-wheeled balancing robot. These models are investigated in this study to find the best controller among the PD, LQR, SMC, and FLC and achieve solid validation. The PD and LQR show a convergence response time of 1.2–2.0 s to the equilibrium state for distance and time, which is slower than the SMC and FLC. The intersection to the equilibrium zone is 1.8 s and 1.2 s, respectively. The angle position response of the PD is 2.5 s, which is slower than the others. Whereas the LQR, SMC, and FLC reach equilibrium in 1.5, 1.5, and 1.25 s, respectively. According to the results, the FLC performed better in two-wheeled auto-balancing under the pendulum within the linear distance in centimeters and angle positions in radian.

Keywords: Two-Wheeled Auto-Balancing Robot, PD Controller, Linear Quadratic Regulator, LQR, Sliding Mode Control, SMC, Fuzzy Logic Control, FLC

LIST OF SYMBOLS

θ	Angular position of the pendulum
$\dot{\theta}$	Angular velocity of the pendulum
$\ddot{\theta}$	Angular acceleration of the pendulum
δ	Boundary layer thickness
x	Position of the robot
$\dot{x}$	Velocity of the robot
$\ddot{x}$	Acceleration of the robot
$e(t)$	Error between the input and output signal
$u(t)$	Control signal
g	Acceleration of gravity
r	Radius of the wheels
M_w	Mass of the wheels
M_p	Mass of the pendulum
I_w	Wheel moment of inertia
I_p	Pendulum moment of inertia
L	Length to the pendulum
K_d	Gain of the differential control
K_p	Gain of the proportional control
K_e	Back-emf constant
K_m	Motor-torque constant
R_a	Motor armature resistance

1. INTRODUCTION

The innovation of two-wheeled balancing robots affects human life in different ways. Such robots come in various types, such as guarding robots, service robots, fire-fighter robots, entertaining robots, and human robots. Immense research continues to be undertaken to make them cheap, efficient, and reliable. Essentially, autonomous mobile robots are two-wheeled, vertical, and self-balancing. Their movements are usually flexible. Two-wheeled robots have a vertical body frame on which all circuitry is placed with a balancing mechanism similar to that of humans. The robot can adjust its position when falling forward or backward to avoid instability. Unlike conventional mobile robots, dual-wheeled, self-balancing robots bring practical advantages.

The elemental control of a two-wheeled balancing robot involves inverted pendulum vision. The inverted pendulum is an emblematic problem in dynamics and control systems. It is a decidedly nonlinear, unstable, and robust coupling structure. The goal is to stabilize

Manuscript received on January 30, 2022; revised on May 13, 2022; accepted on May 30, 2022. This paper was recommended by Associate Editor Matheepot Phattanasak.

[1]The author is with the Department of Robots and Smart Electronics Engineering, Faculty of Engineering and Industrial Technology, Phetchaburi Rajabhat University, Phetchaburi, 76000, Thailand.

[2]The author is with the Department of Industrial Technology and Innovation Management, Faculty of Science and Technology, Pathumwan Institute of Technology, Bangkok, 10330, Thailand.

[†]Corresponding author: c.kritchanan@gmail.com

Digital Object Identifier: 10.37936/ecti-eec.2022203.247520

the pendulum vertically on a motor-driven carriage. It is extensively used as a yardstick to evaluate control techniques (PID controllers, fuzzy control state-space representatives, hereditable algorithms, neural grids, and more). However, the discovery of techniques for controlling and responding to the movement and balancing two-wheeled robots remains a challenge due to the presence of components such as insecurity, multivariable, and nonlinearity.

The controlling logic of the mechanical system is commonly attributable to the simple configuration and contemporary use of reaction or inertia wheels. The conception of maintaining the angular position to change the robot's direction is considered in this case. Control logic is used to understand the behavior of balanced systems and manage environmental interruptions and control methodologies to steady the system. One possible application for this robot is jumping since its wheels and inverted pendulum in the heading direction can be manipulated. Hence, the robot has the aptitude to adjust its functions to achieve the preferred movement and direction. The perception of controlling mechanical systems using reaction wheels or inertia wheels has been reported in a research article by Jepsen *et al.* [1].

The two-wheeled balancing robot has improved momentum and positioning due to the design of nonlinear and unstable dynamic systems over recent decades. The control strategies proposed by developers and researchers allow the two-wheeled balancing robot to control its balance. The two-wheeled balancing robot positioning equipment provides a suitable platform for researchers to investigate the efficiency of various controllers—the two-wheeled balancing robot is based on the inverted pendulum model. Accordingly, a two-wheeled balancing robot needs an excellent controller to enable it to control itself in the appropriate position without directives from the external environment. The movement of a two-wheeled balancing robot is ruled by an under-actuated arrangement, such as the number of control input being less than the number of degrees of freedom requiring stabilization.

Isidori *et al.* [2] demonstrated the degrees of freedom input to be stabilized. For these reasons, researchers have increasingly endeavored to design control systems that guarantee stability and robustness for mobile wheeled inverted pendulums. Although two-wheeled balancing robots are naturally nonlinear with nonlinear differential equations used to describe their dynamics, obtaining a liberalized system model is often possible. Supposing the system works around an operating point and the signals involved are small, a linear model approximates the controlling techniques for obtaining the state of the process in a nonlinear system.

System developers or researchers have applied several techniques to linear systems to design suitable controllers and analysis methods. For example, motion control was proposed using a linear state-space model [3]. In small autonomous helicopters [4], research has been undertaken to provide a low-cost, low-weight attitude estimation system (AES) with a high bandwidth based on a three-axial rate gyro, two-axis inclinometer, and compass. Dynamic control strategies have been studied for the balancing of the robot distance position. The rotation angles of two-wheeled robots were the variables of interest, and a linear controller designed for stabilization by considering the Kalman rank test for controllability, as indicated in the reports of Salerno and Angeles [5, 6].

A two-wheeled self-balancing robot usually consists of two wheels connected to a body frame which holds the motor drive, power and control electronics, and a battery. Sun and Gan [7] managed to keep the robot's behavior predictable by analytical means by reducing the non-uniform distributed mass within the body to point masses. A mathematical model was derived using Lagrangian mechanics based on a whole state feedback controller, combined with two higher-level controls, deployed for stabilization and drive control. A planar model derived a linear stabilizing controller without considering vehicle yaw.

According to Blankespoor and Roemer [8], the aforementioned control laws have been designed on the basis of liberalized dynamics, which only exhibit desirable behavior around the operating point and do not have global applicability. The output tracking was achieved by means of feedback control, with all states remaining in the constraint sets. The general assumption of non-singularity in unknown control coefficient matrices was eliminated using strategic control. The results show that adaptive neural control has been rigorously proven to guarantee the semi-global uniformly ultimate boundedness of all signals in the closed-loop system [9]. The partial feedback was linearized, and a stabilizing position controller and the velocity of the two-wheeled balancing robot derived. However, the controller design is not robust in terms of parameter uncertainty [10]. The PID and LQR schemes involve a two-wheeled balancing robot.

The mathematical model of the two-wheeled balancing robot system has been presented in the form of differential equations. A dynamic model of the system with permanent magnet DC motors included has been derived based on the model proposed by Grasser *et al.* [11]. The responses from the nonlinear two-wheel balancing robot were presented in the time domain. A comparative assessment of both controls was reported in Nasir *et al.* [12]. Controller logic using SMC [13] and fuzzy logic [14] was proposed to ensure robustness versus parameter uncertainty for controlling both the position and rotating angle of the balancing robot. Moreover, Pawananont and Leephakpreeda [15, 16] used control strategies for pulse-width modulation control via Simulink, which Charoensuk *et al.* [17] used to simulate and predict intracranial pressure using clinical data and research articles.

This study focuses on identifying the appropriate

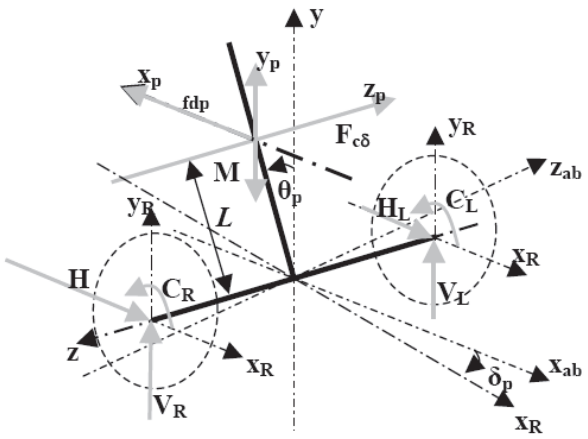

***Fig. 1**: Free body diagram of the two-wheeled balancing robot.*

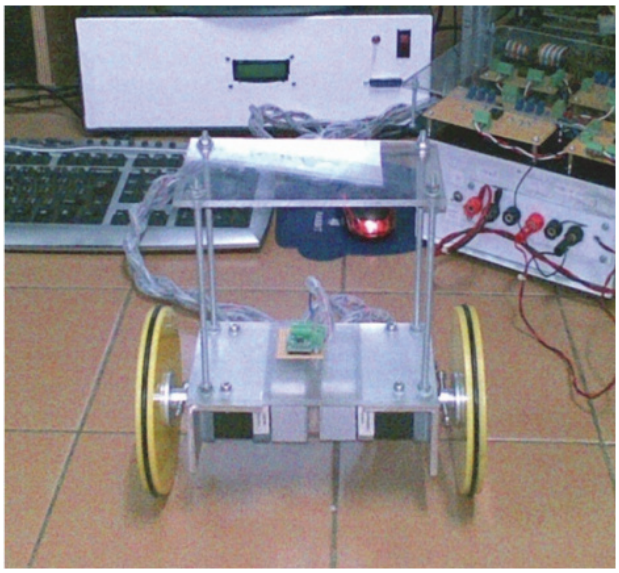

***Fig. 2**: Physical formation of the two-wheeled balancing robot.*

control logic for stabilizing the two-wheeled robot by creating a physical plan of a two-wheeled balancing robot to find the transfer function. The performance of the PD controller, LQR, SMC, and FLC is compared in terms of distance position and rotation angles. Simulink is used to generate the control function. The mathematical model of the two-wheeled balancing robot is presented in the form of differential equations. Finally, the four controller strategies are compared to discover a solid validation model for a two-wheeled balancing robot.

2. MODELING OF THE BALANCING ROBOT

Balancing robots have unstable system dynamics. They are characterized by balancing on two wheels and spinning on the spot. The dynamic model of a balancing robot in this study was derived using a Newtonian approach based on the chassis being modeled as an inverted pendulum [11]. Fig. 1 shows a free body diagram of the chassis and pendulum.

***Table 1**: Parameter constants for a two-wheeled robot.*

Parameter	Value
K_m	0.3674 N·m/A
K_e	0.7661 V·s/rad
M_p	1.5 kg
M_w	0.2 kg
R_a	14 Ω
r	0.06 m
L	0.05 m
g	9.81 m/s^2
I_w	0.00036 kg·m^2
I_p	0.003278 kg·m^2

The balancing robot consists of an inverted pendulum, two wheels, and a DC electric motor. The DC electric motor drives the balancing robot and helps it to maintain balance. Two wheels help the robot to maintain balance via movement of the wheel forte. The inverted pendulum serves to change the equilibrium point of the robot. The components of the robot are connected via connection devices. The connection equipment contacts the computer while the robot equilibrium consists of analog and digital converters. The robot circuit receives the angle measurement signal from the angle-measuring device, while the accelerometer sends the accelerator signal from the robot to the computer. A digital-to-analog converter transmits the computer's control signal to a zero and span circuit. The zero and span circuit adjusts the voltage gain before it is sent to the DC motor driver circuit of the balancing robot, as shown in Fig. 2.

The concept model of the two-wheeled balancing robot depicted in Fig. 2 apportions the robot's deliberation into three parts: (1) the DC electric motor; (2) the two wheels of the balancing robot; and (3) inverted pendulums. Modeling refers to the process of identifying the principal physical dynamic effects to be regarded in analyzing a system, writing the differential and algebraic equations from the conservative and property laws of the relevant specialization, and declining the equations to a convenient differential equation model.

The preliminary model of this research assumes that the wheels of the equilibrium robot do not flow smoothly. The motion angle of the inverted pendulum is considered to be acceptable. The balancing robot measures the distance between the pivot point and the center of mass in the inverted pendulum. The moment of inertia determined by the robot's equilibrium can collect various parameter constants, as shown in Table 1.

This section defines the modeling of the two-wheeled balancing robot as the basis of a simulation background for the development and assessment of both control systems. In Fig. 1, θ represents the pendulum's angle (rad). The equation of motion is derived, leading to the linear dynamic models, given as

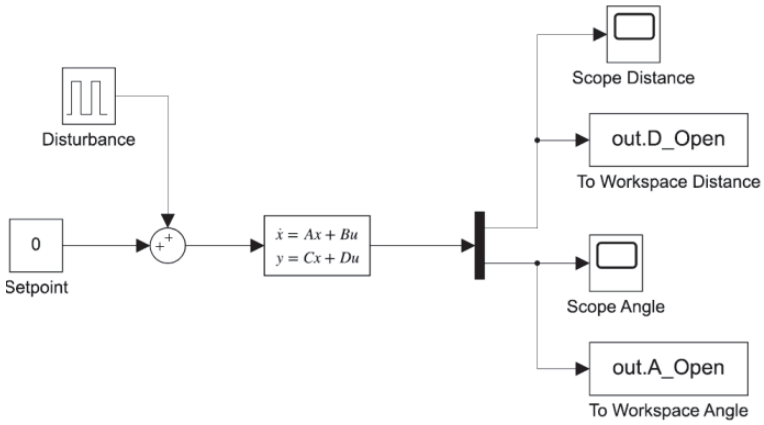

***Fig. 3**: Block diagram of the open-loop system.*

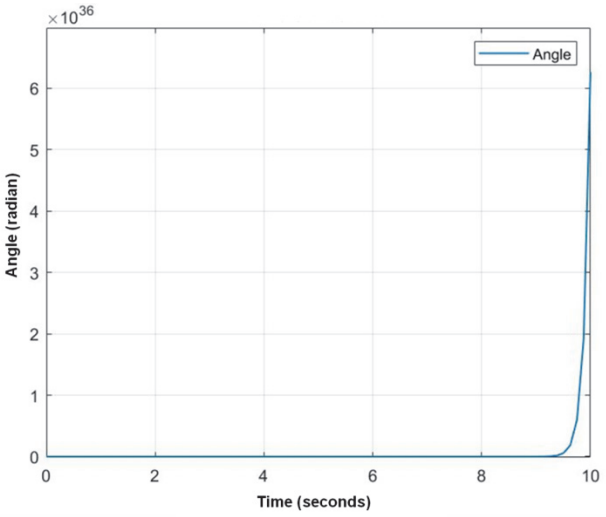

***Fig. 4**: Angular position value of the open-loop system.*

$$\ddot{x} = -\frac{2K_mK_e}{R_ar^2\alpha}\dot{x} - \frac{M_pL}{\alpha}\ddot{\theta}\cos\theta + \frac{2K_m}{R_ar\alpha}V_a + M_pL\dot{\theta}^2\sin\theta \tag{1}$$

$$\ddot{\theta} = \frac{2K_mK_e}{R_ar\beta}\dot{x} - \frac{M_pL}{\beta}\ddot{x}\cos\theta - \frac{2K_m}{R_ar\beta}V_a - \frac{M_pgL}{\beta}\sin\theta \tag{2}$$

where $\alpha = 2M_w + (2I_w/r^2) + M_p$ and $\beta = M_pL^2 + I_p$.

A linearized model can be obtained, and linear state-space controllers designed and implemented $\cos\theta = -1$, $\sin\theta = -\theta$, and $(d\theta/dt)^2 \approx 0$; from Eqs. (1) and (2), the linear equation of motion for the balancing system can be written as

$$\ddot{x} = -\frac{2K_mK_e}{R_ar^2\alpha}\dot{x} + \frac{M_pL}{\alpha}\ddot{\theta} + \frac{2K_m}{R_ar\alpha}V_a \tag{3}$$

$$\ddot{\theta} = \frac{2K_mK_e}{R_ar\beta}\dot{x} + \frac{M_pL}{\beta}\ddot{x} - \frac{2K_m}{R_ar\beta}V_a - \frac{M_pgL}{\beta}\theta \tag{4}$$

By rearranging Eqs. (3) and (4), we get the state-space equation and transfer functions for the system. The state-space equations areas can be written as,

$$\begin{bmatrix}\dot{x}\\ \ddot{x}\\ \dot{\theta}\\ \ddot{\theta}\end{bmatrix} = \begin{bmatrix}0 & 1 & 0 & 0\\ 0 & -2.63 & 2.95 & 0\\ 0 & 0 & 0 & 1\\ 0 & 30.47 & 82.64 & 0\end{bmatrix}\begin{bmatrix}x\\ \dot{x}\\ \theta\\ \dot{\theta}\end{bmatrix} + \begin{bmatrix}0\\ -3.09\\ 0\\ 101.76\end{bmatrix}V_a \tag{5}$$

From Eq. (5), the transfer function is obtained as:

$$\frac{\theta(s)}{V_a(s)} = \frac{101.8s + 173.5}{s^3 + 2.63s^2 - 82.64s - 307.3} \tag{6}$$

The transfer function is applied to the block diagram via Simulink, as shown in Fig. 3. In the subsequent system, the block diagram of the open-loop control system in Fig. 3 gives the input and output signals.

In the block diagram, the system can receive input from the control system to obtain the required output. However, the two-wheeled robot cannot consider this output for additional input reference using this system. Generally, the input provided to the system mainly depends on the required output. Anchored in the input, the controller can generate the control signal and give it to the processing unit. For this reason, based on the control signal, fitting processing can be performed to enable the system to attain output. In the open-loop control system, there is no feedback path.

Accordingly, this is the reason why the input in the open-loop control system is independent of the output. This usually generates a fault within the system. There is no chance of changing the input once the output illustrates the discrepancy from the expected value. In Fig. 4, the angular position based on Eq. (6) with an open-loop system shows the out-of-control signals. This supports that the controller approved the error of output integration with the control system, as expressed in the concept and controller design section.

3. CONCEPT AND CONTROLLER DESIGN

Under impulse interruption, this study investigates a model and controller design for a two-wheeled auto-

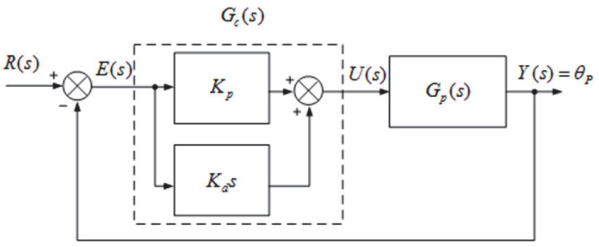

***Fig. 5**: Block diagram of the PD control system.*

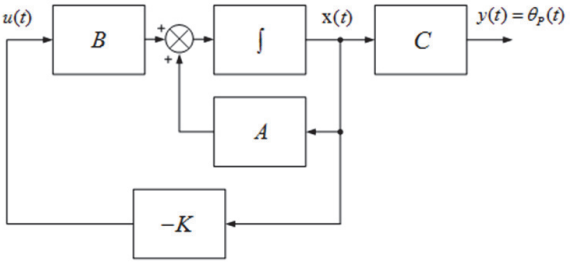

***Fig. 6**: Block diagram of the LQR control system.*

balancing robot. Two-wheeled auto-balancing under the pendulum model is shown in Fig. 1. The control strategies for investigating the state-based controller design in this research are PD, LQR, SMC, and FLC. The input created represents the information as an impulse wave. The controller is simulated via Simulink and satisfies the stability requirement of a two-wheeled auto-balancing robot since it is capable of maintaining the robot's linear position and angle under impulse interruption.

3.1 PD Controller

The PD controller improves the balance element of the robot control system, providing a better instantaneous response with a simple computational structure. Therefore, the PD control can be depicted as a block diagram, as shown in Fig. 5.

From the structure of the PD control system in Fig. 5, the control signal can be written as,

$$u(t) = K_p e(t) + K_i \int e(t)dt + K_d \frac{d}{dt} e(t) \tag{7}$$

The control system uses a PD controller design to stabilize the robot's equilibrium, using the method of placing polls by reducing the output signal in the control system at quarterly rates (quarterly-decay). The second crest is measured against the first crest with the highest response value by the robot's equilibrium control system, and the oscillation of the output waveform equals one-quarter [18].

3.2 LQR Controller

Considering the LQR control model in the system equations as

$$\dot{x} = Ax + Bu \tag{8}$$

Determine the matrix K of the optimal control vector

$$u(t) = -Kx(t) \tag{9}$$

To minimize the performance index

$$J = \int_0^\infty \left(x^* Q x + u^* R u\right) dt \tag{10}$$

where Q and R are positive-definite Hermitian. The matrices Q and R determine the relative importance of the error and expenditure of this energy. It is assumed that the control vector $u(t)$ is unconstrained. The linear control lawgiver, according to Eq. (10), is the LQR control. Therefore, if the matrix's unknown elements K are determined to minimize the performance index, then $u(t) = -Kx(t)$ is optimal for any initial state $x(0)$. A block diagram showing the optimal configuration is shown in Fig. 6.

$$\dot{x} = Ax - BKx = (A - BK)x \tag{11}$$

In the following derivations, it is assumed that the matrices $A-BK$ are stable or that the eigenvalues $A-BK$ have genuine negative parts.

$$\begin{aligned} J &= \int_0^\infty \left(x^* Q x + x^* K^* R K x\right) dt \\ &= \int_0^\infty x^* \left(Q + K^* R K\right) x dt \end{aligned} \tag{12}$$

Following the discussion to solve the parameter-optimizing problem, we set

$$x^* \left(Q + K^* R K\right) x = -\frac{d}{dt}\left(x^* P x\right) \tag{13}$$

where P is a positive-definite Hermitian, the following can be obtained

$$\begin{aligned} x^* \left(Q + K^* R K\right) x &= -x^* P x - x^* P x \\ &= -x^* \left[(A - BK)^* P + P(A - BK)\right] \end{aligned} \tag{14}$$

Comparing both sides of the last equation and noting that it must hold for any x, the following is required

$$(A - BK)^* P + P(A - BK) = -\left(Q + K^* R K\right) \tag{15}$$

Hence, the procedure determines the elements P from this equation and to establish if it is positive or definite. The performance index J can be evaluated as,

$$\begin{aligned} J &= \int_0^\infty x^* \left(Q + K^* R K\right) x dt = -\left. x^* P x \right|_0^\infty \\ &= -x^*(\infty) P x(\infty) + x^*(0) P x(0) \end{aligned} \tag{16}$$

Since all eigenvalues $A - BK$ are assumed to have genuine negative parts, then $x(\infty) \rightarrow 0$ Therefore, the following equation can be obtained

$$J = x^*(0)Px(0) \tag{17}$$

Thus, the performance index J can be obtained based on the initial condition $x(0) = P$. To obtain the solution to the LQR control, the procedure is as follows: Since R the robot has been assumed to be a positive-definite Hermitian or real symmetric matrix and can be written as,

$$R = T^*T \tag{18}$$

where T is a non-singular matrix. Then Eq. (15) can be written as,

$$\left(A^* - B^*K^*\right)P + P(A - BK) + Q + K^*T^*TK = 0 \tag{19}$$

This can be rewritten as,

$$A^*P + PA + [TK - (T^*)^{-1}B^*P]^*[TK - (T^*)^{-1}B^*P] - PBR^{-1}B^*P + Q = 0 \tag{20}$$

The minimization J with respect to K requires the minimization of

$$x^*[TK - (T^*)^{-1}B^*P]^*[TK - (T^*)^{-1}B^*P]x \tag{21}$$

Since this last expression is non-negative, the minimum occurs when it is zero or when

$$TK = (T^*)^{-1}B^*P \tag{22}$$

Hence,

$$K = T^{-1}(T^*)^{-1}B^*P = R^{-1}B^*P \tag{23}$$

Eq. (17) gives the optimal matrix K. Thus, the optimal control law to address the quadratic optimal control problem when the performance index given by Eq. (10) is linear can be written as,

$$u(t) = -Kx(t) = -R^{-1}B^*Px(t) \tag{24}$$

The matrix P in Eq. (23) must satisfy Eq. (15) or the following reduced equation:

$$A^*P + PA - PBR^{-1}B^*P + Q = 0 \tag{25}$$

3.3 SMC Controller

The SMC follows the concept of variable structure control (VSC). This approach was initially introduced at the beginning of the 1950s and has subsequently received considerable attention from researchers, who tend to employ it in different applications and benefit from its numerous advantages. The first step in designing an SMC is to identify the required behavior of the tested system, represented by the sliding surface of the controller. In the current research, the sliding surface of the suggested SMC design is expressed in Eq. (26).

$$S(t) = K_1\ddot{e}(t) + K_2\dot{e}(t) + K_3e(t) + K_4\int e(t)dt \tag{26}$$

where $e(t)$ is the tracking error variable, while K_1, K_2, K_3, and K_4 are the parameters that optimize the transfer function. From a control perspective, it is essential to maintain the tracking signal $e(t)$ and its derivatives equal to zero. Additionally, to keep $S(t)$ at a specified value, it is necessary to maintain its derivative equal to zero, as illustrated in Eq. (27).

$$\dot{S}(t) = 0 \tag{27}$$

The control law of the proposed design illustrated in Eq. (28) is selected by taking into account the condition expressed in Eqs. (26) and (27).

$$U(t) = U_C(t) + U_D(t) \tag{28}$$

where $U_C(t) = F(x(t), r(t), e(t))$; in which $x(t)$ is the control signal, $r(t)$ is the reference signal, and $e(t)$ is the error signal. The term $U_D(t)$ can be expressed in Eq. (29).

$$U_D(t) = K_D\frac{S(t)}{|S(t)| + \delta} \tag{29}$$

Accordingly, the proposed SMC design comprises four parameters. The transfer function finds the optimal values of these parameters by minimizing the integral time absolute error of the deviation in the linear distance and angular positions.

3.4 Fuzzy Controller

The fuzzy controller fragments are as follows: the system has two inputs (Error and d(error)) and one output (output). The error utilizes three fuzzy batches (Neg: Negative, Zero, and Pos: Positive), as shown in Fig. 7. The d(error) uses two fuzzy scenarios (Decrease and Increase), as shown in Fig. 8. The output has three batches (Neg: Negative, Zero, and Pos: Positive), as shown in Fig. 9. The control system later adjusted the fuzzy set limits for functional performance, as defined in Section 4. The fuzzy rules are summarized in Table 2.

4. RESULTS AND DISCUSSION

The control strategies used in this research consist of the PD controller, linear quadratic regulator (LQR), sliding mode control (SMC), and fuzzy logic control (FLC). The hybrid experiment includes physical components and simulation. The four control strategies demonstrate an instantaneous response and resistance to changes in system simulation parameters while also preventing interference from entering the system. A comparative performance assessment of the four control strategies is also discussed in detail in this section.

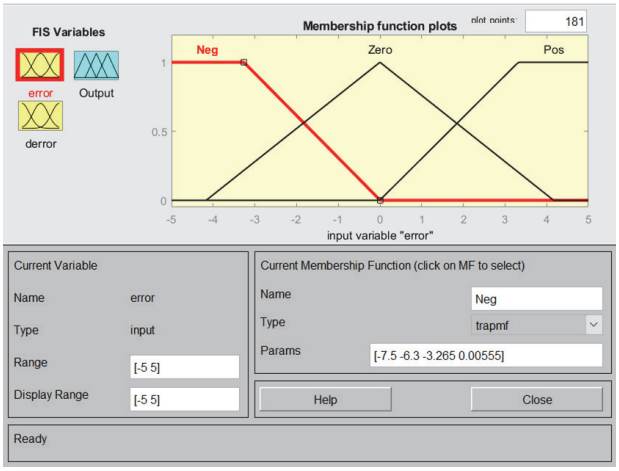

***Fig. 7**: Fuzzy sets for error (Error).*

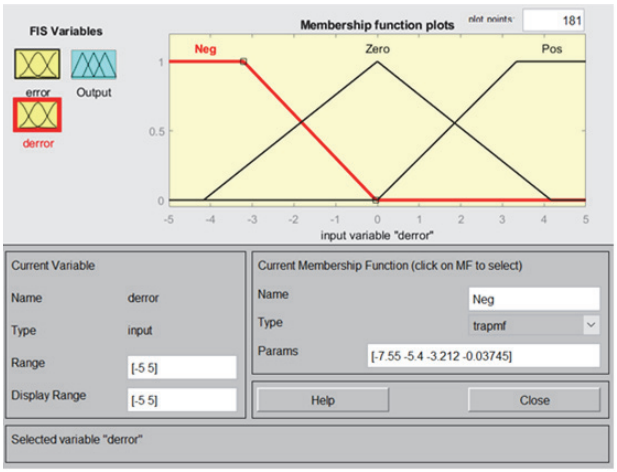

***Fig. 8**: Fuzzy sets for derivative of error (d(error)).*

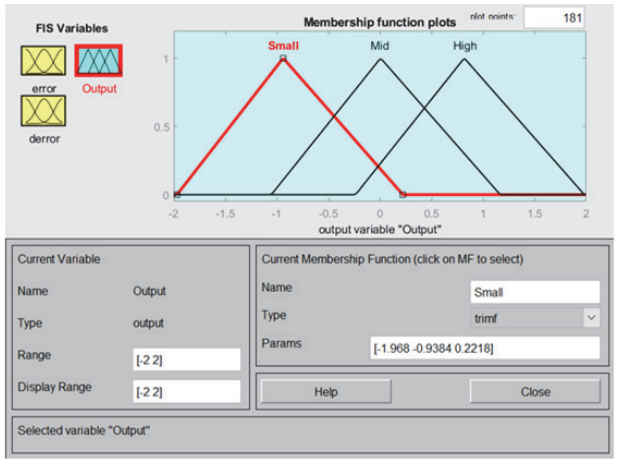

***Fig. 9**: Fuzzy sets for output (Output).*

The input is the impulse wave shown in Fig. 10, which has an amplitude of 1 cm for 0.2 s. The input is a simulator, following the robot's movement when passing a rough surface or the user applied dynamic load. Simulink was used to generate and simulate the control

***Table 2**: Fuzzy rules.*

Condition		Error		
$\frac{d(error)}{dt}$	Input	Neg	Zero	Pos
	Neg	Small	Small	High
	Zero	Small	Mid	High
	Pos	High	High	High

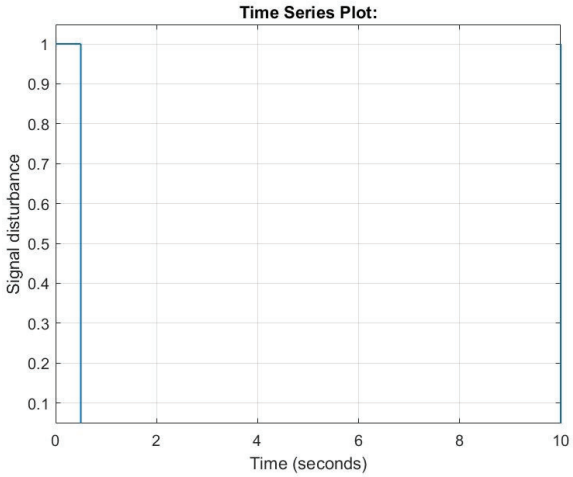

***Fig. 10**: Impulse interruption diagram.*

logic. A block diagram of the four control strategies is shown in Figs. 11(a) for PD controller, 11(b) for LQR controller, 11(c) for SMC controller, and 11(d) for FLC controller.

The two-wheeled balancing robot systems with PD, LQR, SMC, and FLC control strategies shown in the block diagram shape two responses: angular position θ and linear distance position x. As stated earlier, the initial value of the angular position θ in the balancing robot was set to 0.0–1.0 rad while the linear distance position started at the original position $x = 0$ cm. This means that the initial condition of the robot is precarious, and the result of control strategies demonstrates the generation of relationships between angle (rad) versus times (s), as shown in Fig. 12(a) and liner distance positions (cm) versus times (s), as shown in Fig. 12(b). The response time rustles of each control logic are PD (blue line), LQR (red line), SMC (yellow line), and FLC (purple line). The parameter values of the four control logics are investigated by trial and error. They were obtained and summarized for a two-wheeled robot using PD, LQR, and SMC control, as shown in Table 3, and the FLC control rules and fuzzy rule surface in Figs. 13(a) and 13(b), respectively.

The results of the linear distance positions in Fig. 12(b) are summarized in Table 4, demonstrating a comparison of the performance characteristics. The LQR has the fastest settling time of 2.0 s, while PD has the slowest at 6.0 s. The FLC exhibits the best conservation of the linear distance position value of 0.09 cm, the same time as the PD, which has a slip-up distance from the original

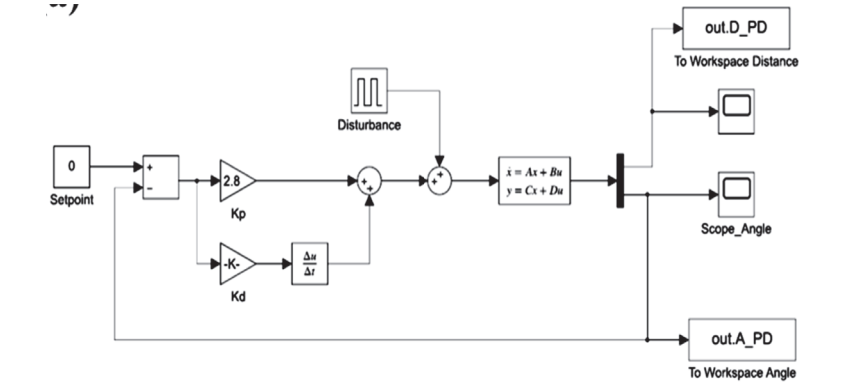

(a)

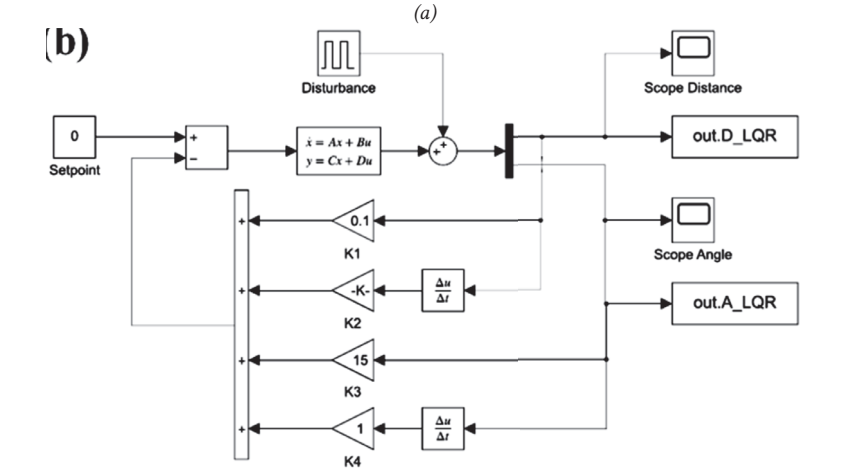

(b)

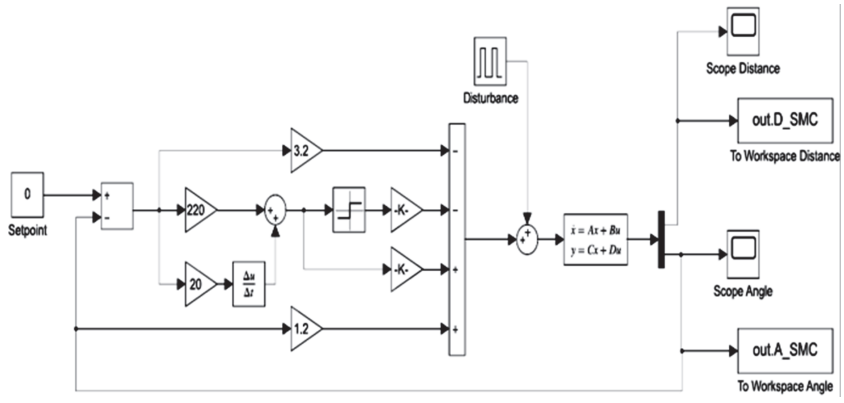

(c)

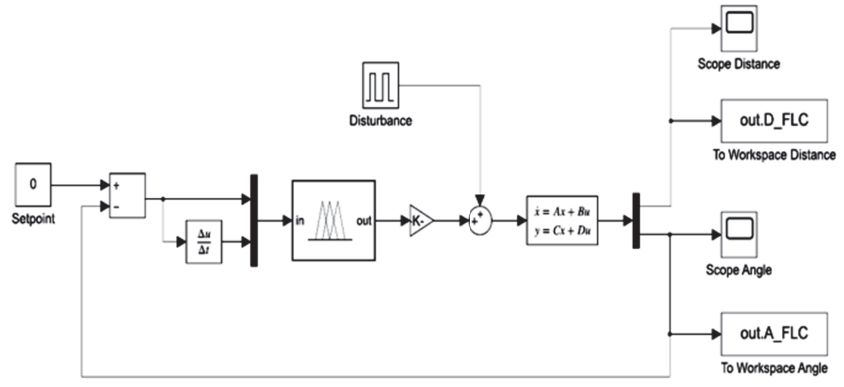

(d)

***Fig. 11**: Block diagrams of the two-wheeled balancing robot: (a) PD, (b) LQR, (c) SMC, and (d) FLC.*

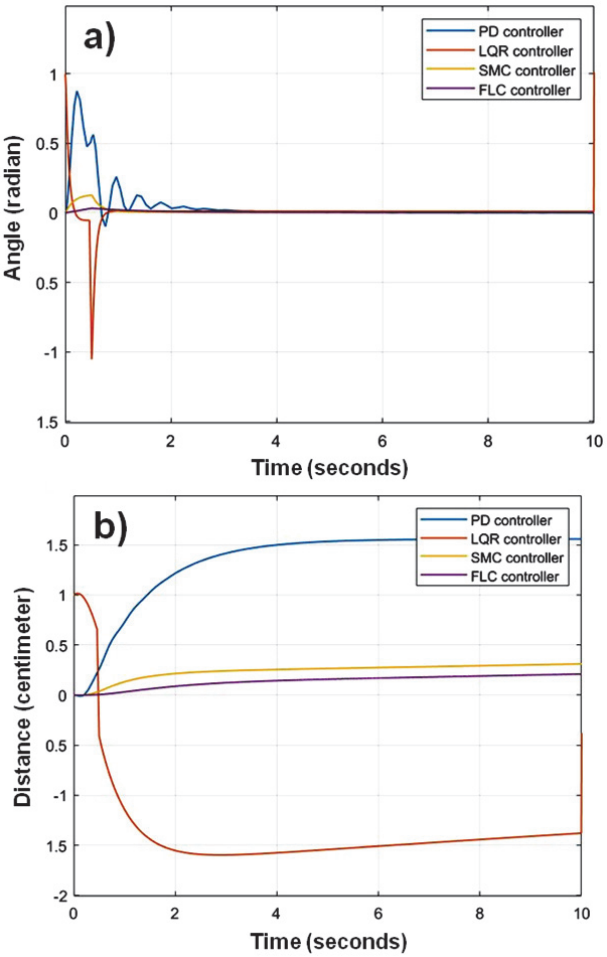

***Fig. 12**: Result among PD, LQR, SMC, and FLC in (a) angular positions and (b) linear distance positions.*

***Table 3**: The controller parameters of PD, LQR, and SMC.*

PD	K_p	2.80
	K_d	0.027
LQR	K_1	0.10
	K_2	0.380
	K_3	15.00
	K_4	1.00
SMC	K_1	3.20
	K_2	220.0
	K_3	20.00
	K_4	1.20
	δ	0.02

position of 1.52 cm. Moreover, the LQR shows harmonic movement with a distance value of 1.00–1.42 cm. Despite the high values for the distance positions, the FLC controller carries itself to a stable position. The balancing robot with the LQR controller exhibits the fastest rise time of 0.2 s. The balancing robot with an FLC controller needs an extra 0.3 s to rise from 10 to 90% to the highest peak linear distance position. These results are similar to

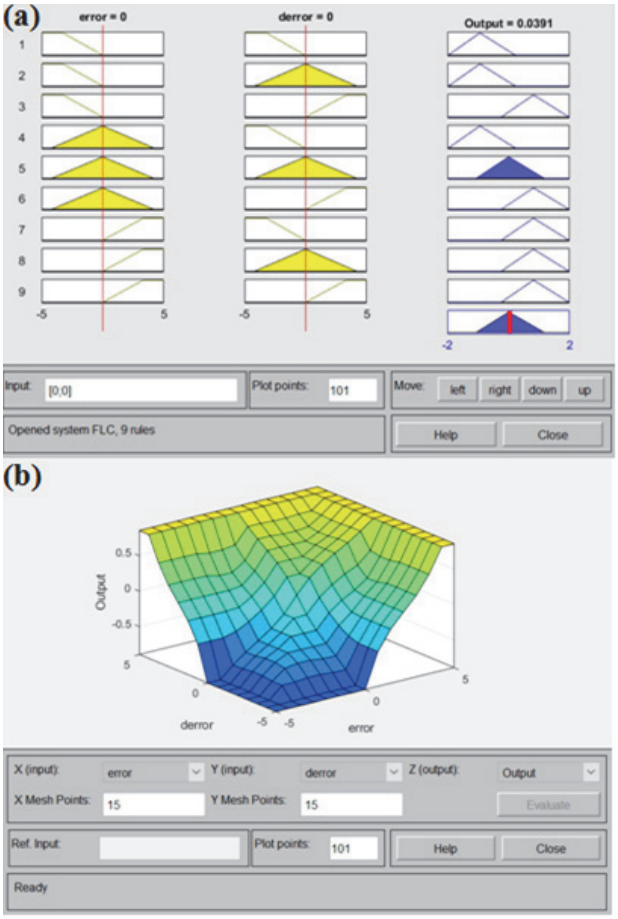

***Fig. 13**: Fuzzy control logic of the two-wheeled balancing robot: (a) fuzzy rule and (b) fuzzy rule surface.*

those reported by Wu *et al.* [14] and Chouhan *et al.* [19]. In the case of steady-state error, almost all controllers demonstrate outstanding performance, giving zero error at 0.7 s and more. The responses of the balancing robot linear distance position exhibit acceptable overshoot and undershoot.

In addition, the results for the settling time value represent the time taken to approach the phase. The rise time in the linear distance positions is shown in Table 4. It can be observed that the LQR provided little value at 0.2 s, while the bulky value of the PD control is 2.0 s. The SMC and FLC gave the same value of 0.5 s. The LQR exhibits the best response, the PD the poorest, and SMC and FLC moderate responses. The results for the settling time value represent the time taken to approach the equilibrium state in each control system. The FLC exhibits the lowest settling time value, followed by SMC, LQR, and PD, respectively, as shown in Table 3. The results are similar to those reported by Yue *et al.* [20] and Bature *et al.* [21].

The results of the angular positions presented in Fig. 12(a) are summarized in Table 5, along with a comparison of the performance characteristics. The FLC exhibits the fastest settling time of 1.52 s and PD the slowest at 6.0 s. The FLC shows the best angular position

***Table 4**: Performance characteristics of a two-wheeled balancing robot: linear distance positions.*

Control Strategies	PD	LQR	SMC	FLC
Rise time (s)	2.0	0.2	0.5	0.5
Settling time (s)	6.0	2.0	1.8	1.2
Steady time error (s)	0.0	0.0	0.0	0.0
Upper limit (cm)	1.52	1.00	0.27	0.09
Lower limit (cm)	0.00	−1.42	0.00	0.00

***Table 5**: Performance characteristics of a two-wheeled balancing robot: angular positions.*

Control Strategies	PD	LQR	SMC	FLC
Rise time (s)	0.2	0.1	0.1	0.1
Settling time (s)	2.5	1.5	1.5	1.25
Steady time error (s)	0.0	0.0	0.0	0.0
Upper limit (cm)	0.98	1.00	0.14	0.01
Lower limit (cm)	−0.10	−1.00	0.00	0.00

conservation value of the linear distance position at 0.01 rad, while the PD and LQR exhibit a more significant angular position from the original of between 1.00 and −1.00 rad. The SM control exhibits a moderate value in an angular position at 0.14 rad. The results for PD control align with those reported by Mahler and Haase [22] and Gonzalez *et al.* [23]. Concerning steady-state error, almost all controllers exhibit an outstanding performance by giving zero error at 0.2 s and more. The responses of the balancing robot angular position show acceptable overshoot and undershoot. The FLC controller carries itself to the initiation position of the angle. The balancing robot with the FLC controller exhibits the fastest rise time of 1.25 s. The results are similar to those reported by Yong *et al.* [24] and Zhang *et al.* [25]. The two balancing robots with a PD controller need 0.1 s more to rise from 10 to 90% to reach the highest peak linear distance position in comparison to LQR, SMC, and FLC control strategies.

In addition, the settling time value results represent the time taken to approach the phase. The rise time in the angular positions presented in Table 5 indicates that the LQR, SMC, and FLC gave a small value of 0.1 s, and the PD control a bulky value of 0.2 s, while the LQR, SMC, and FLC gave the same value of 0.1 s. The LQR, SMC, and FLC exhibit the best response in the angular position state while the PD shows a poor response. The settling time value results represent the time taken to approach the equilibrium state of each control system. The settling time value shows that the lowest value of the responses for each controller is plotted in one window, as summarized in Tables 4 and 5. The PD and LQR exhibit a response time convergence of 1.2–2.0 s to reach equilibrium according to the distance and time diagram, which is slower than SMC and FLC. The intersection to the equilibrium zone is 1.8 s and 1.2 s, respectively. The PD exhibits a settling time of 2.5 s, meaning that it is slow to reach the equilibrium state.

Incidentally, the angle response of PD is 2.5 s slower than LQR, SMC, and FLC, which exhibit values of 1.5, 1.5, and 1.25 s, respectively. The angle response of the LQR and SMC control converge at the time value. The results indicate that these are better controllers than PD and FLC for achieving a solid validation. Despite the LQR demonstrating a virtuous rise time, the results show that the FLC achieves the best performance in two-wheeled auto-balancing under the equilibrium state, with the inverted pendulum being within the linear distance in cm and angle positions in rad, as presented in Fig. 12. The FLC exhibits the best response behavior for to control stabilizer, aligning with the results of previous research [1, 7, 12, 19, 26–29]. The four logical controls obtained zero for the steady-state time error.

5. CONCLUSION

In conclusion, the designs of the PD, LQR, SMC, and FLC are presented and compared in this study. These four controllers perform stabilization functions to enable the robot to maintain its balance. When designing the four controllers, the mathematical model of the equilibrium robot must first be determined. In this research, Newton's laws are applied in the design. A mathematical model of a balancing robot is mainly used for design considerations. The mathematical model of an equilibrium robot is determined according to the total kinetic energy of the system.

Nevertheless, the mathematical model of an equilibrium robot derived from Newton's laws is a nonlinear system. Hence, the controller must first convert the mathematical model of the nonlinear equilibrium robot into a linear one. In this study, a mathematical model of a linear equilibrium robot was applied to the controller design. In simulations and experiments, the ability of the controller is used to stabilize the balancing robot. The system of the balancing robot is simulated using the actual structure of the controller and comparing the performance of the inverted pendulum angle in the balancing robot with the controller obtained from the mathematical model. Equilibrium is reached by comparing the angle and distance performance values of the balancing robot control system using the PD LQR, SCM, and FLC. A PD controller is used to control the balancing robot system along with the LQR, SLM, and FLC. In the equilibrium state, these four controllers derived from the linear equations of mathematical models can be used to control and maintain the stability of balancing robots. Nevertheless, the four controllers take the same time to reach the equilibrium point.

The simulation and experimental results show that a PD controller, LQR, SMC, and FLC can be used to drive an equilibrium robot. As can be observed from the oscillation of the inverted pendulum angle and the position value of the equilibrium robot, the PD controller takes longer to reach the equilibrium point than the LQR.

The SMC and FLC, respectively, can maintain the stability of the balancing robot better than the PD controller. However, the LQR and SMC have many slide mode controls. Moreover, the four control logics have design limitations in transferring from a nonlinear system to a linear control system. The system stabilization response must be developed and the parameters improved to enable the controller to support the nonlinearity of the applied system to respond more effectively and maintain system balance.

REFERENCES

[1] F. Jepsen, A. Soborg, A. R. Pedersen, and Z. Yang, "Development and control of an inverted pendulum driven by a reaction wheel," in *2009 International Conference on Mechatronics and Automation*, 2009, pp. 2829–2834.

[2] A. Isidori, L. Marconi, and O. S. University, *Robust Autonomous Guidance: An Internal Model Approach*. New York, USA: Springer, 2003.

[3] Y.-S. Ha and S. Yuta, "Trajectory tracking control for navigation of the inverse pendulum type self-contained mobile robot," *Robotics and Autonomous Systems*, vol. 17, no. 1-2, pp. 65–80, Apr. 1996.

[4] A.-J. Baerveldt and R. Klang, "A low-cost and low-weight attitude estimation system for an autonomous helicopter," in *Proceedings of IEEE International Conference on Intelligent Engineering Systems*, 1997, pp. 391–395.

[5] A. Salerno and J. Angeles, "The control of semi-autonomous two-wheeled robots undergoing large payload-variations," in *Proceedings of IEEE International Conference on Robotics and Automation (ICRA'04)*, 2004, pp. 1740–1745.

[6] A. Salerno and J. Angeles, "On the nonlinear controllability of a quasiholonomic mobile robot," in *2003 IEEE International Conference on Robotics and Automation*, 2003, pp. 3379–3384.

[7] L. Sun and J. Gan, "Researching of two-wheeled self-balancing robot base on LQR combined with PID," in *2010 2nd International Workshop on Intelligent Systems and Applications*, 2010.

[8] A. Blankespoor and R. Roemer, "Experimental verification of the dynamic model for a quarter size self-balancing wheelchair," in *Proceedings of the 2004 American Control Conference*, 2004, pp. 488–492.

[9] Z. Chen, Z. Li, and C. L. P. Chen, "Adaptive neural control of uncertain MIMO nonlinear systems with state and input constraints," *IEEE Transactions on Neural Networks and Learning Systems*, vol. 28, no. 6, pp. 1318–1330, Jun. 2017.

[10] K. Pathak, J. Franch, and S. Agrawal, "Velocity and position control of a wheeled inverted pendulum by partial feedback linearization," *IEEE Transactions on Robotics*, vol. 21, no. 3, pp. 505–513, Jun. 2005.

[11] F. Grasser, A. D'Arrigo, S. Colombi, and A. Rufer, "JOE: a mobile, inverted pendulum," *IEEE Transactions on Industrial Electronics*, vol. 49, no. 1, pp. 107–114, Feb. 2002.

[12] A. N. K. Nasir, M. A. Ahmad, and R. M. T. R. Ismail, "The control of a highly nonlinear two-wheels balancing robot: A comparative assessment between LQR and PID-PID control schemes," *International Journal of Mechanical and Mechatronics Engineering*, vol. 4, no. 10, pp. 942–947, 2010.

[13] D. Nasrallah, H. Michalska, and J. Angeles, "Controllability and posture control of a wheeled pendulum moving on an inclined plane," *IEEE Transactions on Robotics*, vol. 23, no. 3, pp. 564–577, Jun. 2007.

[14] J. Wu, W. Zhang, and S. Wang, "A two-wheeled self-balancing robot with the fuzzy PD control method," *Mathematical Problems in Engineering*, vol. 2012, 2012, Art. no. 469491.

[15] K. Pawananont and T. Leephakpreeda, "Sequential control of multichannel on–off valves for linear flow characteristics via averaging pulse width modulation without flow meter: An application for pneumatic valves," *Journal of Dynamic Systems, Measurement, and Control*, vol. 141, no. 1, Jan. 2019, Art. no. 011007.

[16] K. Pawananont and T. Leephakpreeda, "Experimental investigation and optimal combustion control of untreated landfill gas via fuzzy logic rule knowledge based approach," *Waste Management*, vol. 121, pp. 383–392, Feb. 2021.

[17] K. Charoensuk, T. Sethaput, and I. Nilkhamhang, "Electrical modeling of dynamical interaction among intracranial pressure, intraocular pressure, cerebral perfusion pressure, and arterial blood pressure," in *2019 12th Biomedical Engineering International Conference (BMEiCON)*, 2019.

[18] C. W. de Silva, *Modeling and Control of Engineering Systems*. Boca Raton, Florida, USA: CRC Press, 2009.

[19] A. S. Chouhan, D. R. Parhi, and A. Chhotray, "Control and balancing of two-wheeled mobile robots using Sugeno fuzzy logic in the domain of AI techniques," in *Emerging Trends in Engineering, Science and Manufacturing (ETESM-2018)*, 2018.

[20] M. Yue, W. Sun, and P. Hu, "Sliding mode robust control for two-wheeled mobile robot with lower center of gravity," *International Journal of Innovative Computing, Information and Control*, vol. 7, no. 2, pp. 637–646, Feb. 2011.

[21] A. A. Bature, S. Buyamin, M. N. Ahmad, and M. Muhammad, "A comparison of controllers for balancing two wheeled inverted pendulum robot," *International Journal of Mechanical & Mechatronics Engineering*, vol. 14, no. 3, pp. 62–68, Jun. 2014.

[22] B. Mahler and J. Haase, "Mathematical model and control strategy of a two-wheeled self-balancing robot," in *IECON 2013 - 39th Annual Conference of the IEEE Industrial Electronics Society*, 2013, pp. 4198–4203.

[23] C. Gonzalez, I. Alvarado, and D. M. L. Peña, "Low cost two-wheels self-balancing robot for control

education," *IFAC-PapersOnLine*, vol. 50, no. 1, pp. 9174–9179, Jul. 2017.

[24] Q. Yong, L. Yanlong, Z. Xizhe, and L. Ji, "Balance control of two-wheeled self-balancing mobile robot based on TS fuzzy model," in *Proceedings of 2011 6th International Forum on Strategic Technology*, 2011, pp. 406–409.

[25] J. Zhang, T. Zhao, B. Guo, and S. Dian, "Fuzzy fractional-order PID control for two-wheeled self-balancing robots on inclined road surface," *Systems Science & Control Engineering*, vol. 10, no. 1, pp. 289–299, 2022.

[26] S. Khatoon, M. Istiyaque, N. Hasan, and D. K. Chaturvedi, "Two-wheeled self-balancing mobile robot using kalman filter and LQG regulator," in *Recent Advances in Mechanical Engineering*, M. Muzammil, A. Chandra, P. K. Kankar, and H. Kumar, Eds. Singapore: Springer, 2021, pp. 213–221.

[27] S. Miasa, M. Al-Mjali, A. A.-H. Ibrahim, and T. A. Tutunji, "Fuzzy control of a two-wheel balancing robot using DSPIC," in *2010 7th International Multi-Conference on Systems, Signals and Devices*, 2010.

[28] L. J. Saud and M. M. Alwan, "Design and implementation of classical sliding mode controller for ball and plate system," *Journal of Engineering*, vol. 23, no. 6, pp. 74–92, 2017.

[29] M. Herrera, P. Leica, D. Chávez, and O. Camacho, "A blended sliding mode control with linear quadratic integral control based on reduced order model for a vtol system," in *Proceedings of the 14th International Conference on Informatics in Control, Automation and Robotics (ICINCO 2017)*, 2017, pp. 606–612.

Kanchit Pawananont received his B.Eng. degree in electrical engineering from Mahanakorn University of Technology (MUT), Thailand, in 2005, and M.Eng. in control engineering from King Mongkut's Institute of Technology Ladkrabang (KMITL), Thailand in 2011 and the Ph.D. degree in engineering and technology from Sirindhorn International Institute of Technology (SIIT), Thammasat University, Thailand in 2021. He is currently a lecturer in department of robots and smart electronics engineering, Phetchaburi Rajabhat University, Thailand. His research interests mainly robotics and automatic control systems.

Kritchanan Charoensuk received his B.Eng. and M.Eng degrees in mechanical engineering from King Mongkut's University of Technology Thonburi (KMUTT), Thailand, in 2011 and 2017 respectively. He is currently a lecturer in the Department of Industrial Technology and Innovation Management, Faculty of Science and Technology, Pathumwan Institute of Technology, Thailand. His research interests mainly materials science and engineering, metal forming process, finite element methods, robotics and automatic control systems.